

Assignments of the Pfr–Pr FTIR Difference Spectrum of Cyanobacterial Phytochrome Cph1 Using ^{15}N and ^{13}C Isotopically Labeled Phycocyanobilin Chromophore

Jasper J. van Thor,^{*,†} Nicholas Fisher,[‡] and Peter R. Rich^{*}

Laboratory of Molecular Biophysics, Rex Richards Building, University of Oxford, South Parks Road, Oxford OX1 3QU, U.K., and Glynn Laboratory of Bioenergetics, Department of Biology, University College London, Gower Street, London WC1E 6BT, U.K.

Received: May 4, 2005; In Final Form: September 2, 2005

The reversible red and far-red light-induced transitions of cyanobacterial phytochrome Cph1 from *Synechocystis* PCC 6803 were investigated by Fourier transform infrared (FTIR) difference spectroscopy. High-quality light-induced Pfr–Pr difference FTIR spectra were recorded for the 58 kDa N-terminal domain of Cph1 by repetitive photochemical cycling and signal averaging. The Pfr–Pr difference spectra in H_2O and D_2O were very similar to those previously reported for full-length 85 kDa Cph1.¹ Published assignments were extended by analysis of the effects of ^{13}C and ^{15}N isotope substitutions at selected sites in the phycocyanobilin chromophore and by ^{15}N global labeling of the protein. The Pfr–Pr difference spectra were dominated by an amide I peak/trough at $1653\text{ cm}^{-1}(+)/1631\text{ cm}^{-1}(-)$ and a smaller amide II band at 1554 cm^{-1} . Labeling effects allowed specific chromophore assignments for the $\text{C}_1=\text{O}$ ($1736\text{ cm}^{-1}(-)/1724\text{ cm}^{-1}(+)$) and $\text{C}_{19}=\text{O}$ ($1704\text{ cm}^{-1}(-)$) carbonyl vibrations, $\text{C}=\text{C}$ vibrations at $1589\text{ cm}^{-1}(+)$, and bands at $1537(-)$, $1512(+)$, $1491(-)$, $1163(+)$, $1151(-)$, $1134(+)$, $1109(-)$, and $1072(-)\text{ cm}^{-1}$ that must involve chromophore C–N bonds. A variety of additional changes were insensitive to isotope labeling of the chromophore. Effects of ^{15}N labeling of the protein were used to tentatively assign some of these to specific amino acid changes. Those insensitive to ^{15}N labeling included a protonated aspartic or glutamic acid at $1734\text{ cm}^{-1}(-)/1722\text{ cm}^{-1}(+)$ and a cysteine at $2575\text{ cm}^{-1}(+)/2557\text{ cm}^{-1}(-)$. Bands sensitive to ^{15}N protein labeling at $1487\text{ cm}^{-1}(+)/1502\text{ cm}^{-1}(-)$ might arise from tryptophan and bands at $1261\text{ cm}^{-1}(+)/1244\text{ cm}^{-1}(-)$ and $1107\text{ cm}^{-1}(-)/1095\text{ cm}^{-1}(+)$ might arise from a histidine environment or protonation change. These assignments are discussed in light of the $15Z\text{--}E$ photoisomerization model of phototransformation and the associated protein conformational changes.

Introduction

After their initial discovery in seedlings in 1959,² phytochromes were shown to be responsible for a wide range of photomorphogenic responses in plants and have also more recently been found in cyanobacteria.³ In plants, three or five different phytochromes may be present which can have overlapping biological functions, contributing to shade avoidance, hypocotyl elongation, seed germination, flowering, and other processes.⁴ The cyanobacterial phytochrome Cph1 from *Synechocystis* PCC 6803 shows red/far-red light-reversible transformations typical of phytochromes and carries a phycocyanobilin (PCB) chromophore. Cph1 belongs to the histidine kinase class of receptor molecules, and light-induced changes in the phosphorylation level of the kinase domain and the interacting response regulator Rcp1 have been demonstrated.³ This implicates phosphoryl transfer in the initial step of light signal transduction by Cph1. The downstream signaling partners of Cph1 and Rcp1 have not yet been identified, but expression of both genes has been detected in the wild-type strain.⁵ With respect to the photochemical and structural basis of signal transduction, Cph1 is considered to be a good model for plant phytochromes as well. Optical, Raman, and FTIR spectroscopic studies on Cph1 have indeed shown the photochemistry in Cph1

to be similar to that of plant phytochromes.^{1,6} The phototransformation from the Pr state to the Pfr state is likely to involve a $Z \rightarrow E$ isomerization at the $\text{C}_{15}=\text{C}_{16}$ bond between the C- and D-rings of the linear tetrapyrrole chromophore (Figure 1), although conclusive evidence is still lacking. NMR measurements have suggested that a chromopeptide prepared from oat phytochrome in the Pfr form has the $15E$ configuration, whereas a peptide derived from the Pr form has a $15Z$ configuration.⁷

The red and far-red light-induced reactions of both plant and cyanobacterial phytochromes have been addressed by resonance Raman and FTIR spectroscopy studies, a selection of which is considered here.^{1,6,8–14} Several of these studies have addressed the vibrational spectroscopy of the photocycle intermediates in the $\text{Pr} \rightarrow \text{Pfr}$ and $\text{Pfr} \rightarrow \text{Pr}$ pathways as well.^{1,10,11,13,14} In Cph1, the meta-Ra and meta-Rc states and the lumi-F and meta-F states have been identified and characterized in the $\text{Pr} \rightarrow \text{Pfr}$ and $\text{Pfr} \rightarrow \text{Pr}$ pathways, respectively.¹

Assignments of the resonance Raman and FTIR spectra have been addressed by comparing the spectra of materials with homologue chromophores^{6,12,13} and using model pigments,^{8,9} isotope substitutions,^{12,13} and mode calculations.¹⁴ In the recombinant oat phytochrome, substitutions in the phycocyanobilin chromophore of the $\text{C}_5\text{--H}$, $\text{C}_{10}\text{--H}$, and $\text{C}_{15}\text{--H}$ H atoms by D isotopes have allowed the assignment of hydrogen out-of-plane (HOOP) modes in the resonance Raman spectra.¹² In particular, a strong peak in the resonance Raman spectra of Pfr at $\sim 820\text{ cm}^{-1}$ has been assigned to the $\text{C}_{15}\text{--H}$ HOOP mode,

* To whom correspondence should be addressed. E-mail: Jasper@biop.ox.ac.uk. Tel: +44 (0)1865 285352. Fax: +44 (0)1865 275182.

[†] University of Oxford.

[‡] University College London.

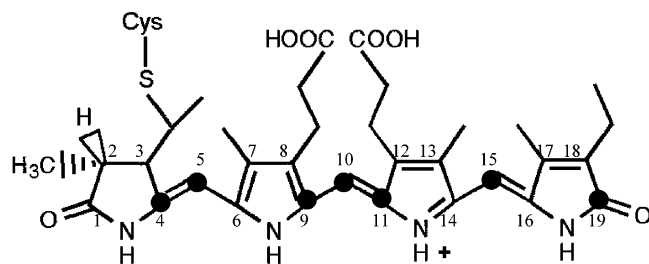


Figure 1. ^{13}C labeling pattern of the phycocyanobilin chromophore. Carbon atoms are numbered according to tetrapyrrole nomenclature. Carbons atoms C4, C5, C9, C10, C11, C15, and C19 indicated with dots are substituted with ^{13}C isotopes in the 5'-aminolevulinic-5- ^{13}C acid derived material. All four pyrrole nitrogens are labeled in the 5'-amino- ^{15}N -levulinic acid derived material.

consistent with a nonplanar conformation of the C- and D-rings in the Pfr state, which has been cited as strong evidence supporting $\text{C}_{15}=\text{C}_{16}$ $Z \rightarrow E$ isomerization.^{9,12} Substitution of the $\text{C}_1=\text{O}$ oxygen with the ^{18}O isotope of the 65 kDa N-terminal fragment of oat PhyA reconstituted with phycocyanobilin (PCB) has allowed the assignment of a peak/trough at $1749\text{ cm}^{-1}(+)/1731\text{ cm}^{-1}(-)$ in the Pfr-Pr FTIR difference spectrum to the unconjugated $\text{C}_1=\text{O}$ bond.¹³ This work also clearly showed the coupling of the $\text{C}_1=\text{O}$ bond to the adjacent N-H bending mode in ring A in phyA, as has previously also been shown for model compounds.⁸ Conjugated $\text{C}=\text{O}$ stretch vibrations were assigned to bands at low frequencies, at 1697 and 1704 cm^{-1} , in the model compounds 2,3-dihydro-2,3,7,8,12,13,17,18-octaethylbilindion (DHBV) and 2,3,7,8,12,13,17,18-octaethylbilindion (OEBV), respectively.⁸ The nonconjugated $\text{C}_1=\text{O}$ stretch vibrations in the model compounds DHBV and protonated PCB were found at 1733^8 and $1735\text{ cm}^{-1,13}$ respectively.

Besides these studies, assignments of vibrational modes have been mostly proposed on the basis of model compound studies and quantum chemical calculations.^{8,14,15} To further develop assignments of the Pfr-Pr FTIR difference spectra of Cph1, we prepared materials containing ^{15}N and ^{13}C isotope substitutions in the chromophore as well as global ^{15}N substitutions and the H/D exchange of the protein plus chromophore. The resultant shifts observed in the FTIR difference spectra have allowed specific assignments to amino acid, chromophore, and global backbone conformational changes. These data can be used in combination with systematic vibrational spectroscopy studies and calculations¹⁴ to shed light on the molecular mechanism of phototransformation and signaling by the phytochrome photoreceptors.

Materials and Methods

Expression and Isotope Substitution. The N-terminal 58 kDa fragment of the *Synechocystis* PCC 6803 phytochrome Cph1 (Cph1-N515) was amplified by polymerase chain reaction (PCR) from a DNA construct containing the *cph1* gene, kindly provided by Clark Lagarias, using primers NCPHNDE (ATATCATATGGCCACCACCGTACAA) and CPH515XHO (AAGTGCTCGAGTTCTTCTGCCTGGCGCAAAT). The product was digested with *NdeI* and *XhoI* and cloned into *NdeI/XhoI* digested pET-22b. The Cph-N515 construct was expressed in *E. coli* BL21(DE3), together with a construct harboring the *Synechocystis* *hoI* and *pcyA* genes encoding heme oxygenase and phycocyanobilin:ferredoxin oxidoreductase, similar to previously reported constructs.¹⁶ To construct this coexpression plasmid, the *hoI* gene was amplified by PCR from genomic DNA from *Synechocystis* PCC 6803 using primers NHO1KPN (GCAGGTACCTGAGTGTCAACTTAGCTTCCCAG) and

CHO1BAM (GCAGGATCCCTAGCCTTCGGAGGTGGC-GAGGCC) and the *pcyA* gene was amplified using the primers NPCYANCO (GATCCATGGCCGTCACTGATTTAAGTTTG) and CPCYAKPN (GCAGGTACCATTCTCCTTCTGCTTT-TATTGGATAACATCAAATAAG). The products were digested with *KpnI* and *BamHI* and *KpnI* and *NcoI*, respectively, and ligated together into a *BamHI/NcoI*-digested ColE1-compatible vector pMR101.¹⁷ Expression of a bicycronic transcript containing the *hoI* and *pcyA* genes from pMR101 is controlled by a T7 promoter. Cph1-N515 was expressed at 30°C , resulting in typical yields of $100\text{--}120\text{ mg/L}$.

An aminolevulinic acid (5-ALA) auxotrophic BL21(DE3) strain was created by insertion mutagenesis of the *hemA* gene encoding glutamyl-tRNA reductase.¹⁸ The *hemA* gene was amplified from genomic DNA from *E. coli* BL21(DE3) as a 1249 bp PCR product using the primers NHEMABAM (AGACGGATCCCTTTTAGCACTCGGTATC) and CHEMAE-CO (CGAGGAATTCGCGAGAATATTCAGGC). The product was digested with *EcoRI* and *BamHI* and cloned into the *EcoRI/BamHI* digested conditional origin from R6K¹⁹ and transformed to *E. coli* DH5 α - λ pir. An internal 261 bp fragment was excised from the *hemA* clone with *EcoRV* and replaced with a 1489 bp *EcoRV/XmnI* fragment containing the Cm-r cassette from pACYC-duet (Novagen). The resulting construct was linearized with *EcoRI* and electroporated to *E. coli* BL21(DE3). Transformants were selected on selective plates containing $100\text{ }\mu\text{M}$ 5'-aminolevulinic acid (Sigma) and $30\text{ }\mu\text{g/mL}$ of chloramphenicol. A *hemA* mutant was selected from the lack of growth on media lacking 5'-aminolevulinic acid. For incorporation of ^{13}C and ^{15}N isotopic labels into the chromophore, *E. coli* BL21(DE3)::*hemA* (pET22b-*cph*-N515) (pMR101-*pcyA*-*hoI*) was grown at 30°C in the presence of 0.5 mM 5-aminolevulinic-5- ^{13}C acid (Isotec) or 0.5 mM 5-amino- ^{15}N -levulinic acid (CDN Isotopes), respectively. ^{15}N labeling of the protein was achieved by expression in Martek 9-N medium (Spectra Stable Isotopes).

Phytochrome was purified by metal chelate affinity chromatography using Ni-NTA resin (Sigma) and subsequent purification by Superdex 200 gel filtration chromatography (Amersham Biosciences). Sample conditions were adjusted to 4 mM Tris/HCl pH 7.8.

FTIR Spectroscopy. Samples in 4 mM Tris/HCl pH 7.8 were concentrated to $2\text{--}3\text{ mM}$ concentration in either H_2O or D_2O and $2\text{--}3\text{ }\mu\text{L}$ aliquots and were placed between 2 cm diameter CaF_2 windows and sealed with vacuum grease. Optimal sample concentration gave a combined absorbance peak of water and protein at 1655 cm^{-1} of $0.9\text{--}1.1$. The sample temperature was maintained at 15°C during FTIR data acquisition, which were recorded with a Bruker IFS 66/S spectrometer equipped with a liquid-nitrogen-cooled MCT-A detector. A measurement cycle began with 20 s far-red preillumination at approximately $2.5 \times 10^{-4}\text{ E}\cdot\text{m}^{-2}\cdot\text{s}^{-1}$ provided by a far-red LED ($\lambda_{\text{em}} = 735\text{ nm}$, Quantum Devices, P/N QDDH73502, operated at 20 mA , 4.06 mW) placed within 1 cm of the sample surface, after which 200 interferograms were averaged to provide a background scan. The LED was then switched off, and actinic red light at $15\text{ W}\cdot\text{m}^{-2}$ was provided for 2 s by a fiber optic from a quartz-iodine source filtered with a 680 nm cutoff, glass heat, and water filters. A sample scan of 200 interferograms was recorded 1 s after switching off this light source. Batches of 50 cycles were averaged and stored temporarily in order to check stability and reproducibility. The spectra shown are the final averages of several thousand individual cycles run over several days, during which time no loss or changes of signals were apparent. IR spectra were measured with a resolution of 4 cm^{-1} , and quoted

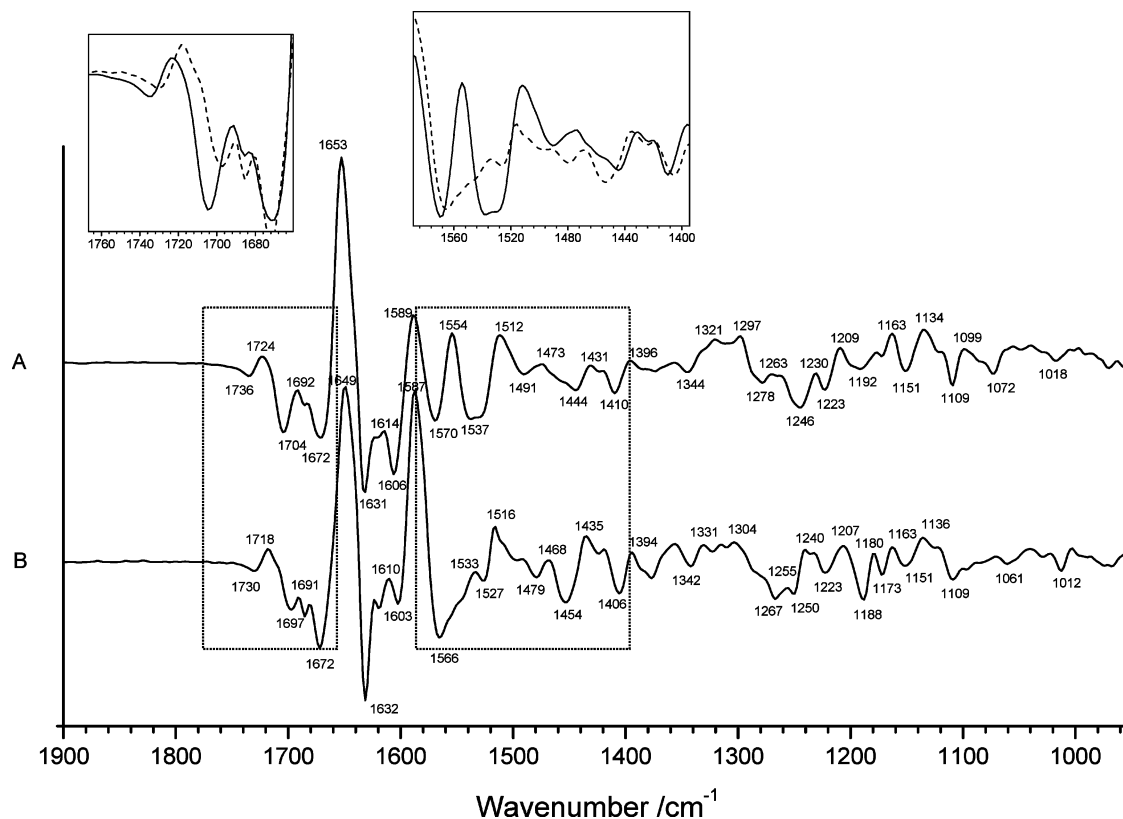


Figure 2. Pfr–Pr FTIR difference spectrum in H₂O and D₂O. Difference spectra in (A) H₂O and (B) D₂O. Insets show overlays of the data in H₂O (solid line) and D₂O (dotted line) and also show overlays of regions with band position changes that are discussed.

frequencies have an accuracy of $\pm 1 \text{ cm}^{-1}$. For measurements in deuterium oxide (D₂O), identical D₂O buffers at pD 7.8 were prepared assuming $\text{pD} = \text{pH}_{\text{reading}} + 0.4$ ²⁰ and buffer exchange was achieved by several cycles of centrifugal concentration and buffer replacement. The extent of H/D exchange was estimated to be >90% using the method described in Rath et al.²¹

Results and Discussion

Expression, H/D Exchange, and Isotope Labeling. The holo-form of the N-terminal 58 kDa fragment Cph-N515 was produced following a procedure involving coexpression of the heme oxygenase and bilin reductase genes from *Synechocystis* PCC 6803, similar to a published method.¹⁶ Expression of Cph-N515 using the 5'-ALA auxotrophic *hemA* mutant strain in the presence of 0.5 mM 5-aminolevulinic-5-¹³C acid (Isotec) or 0.5 mM 5-amino-¹⁵N-levulinic acid (CDN isotopes) achieved complete isotopic substitutions in the chromophore. The ¹³C labeling pattern resulting from the use of 5-aminolevulinic-5-¹³C acid is shown in Figure 1. The labeling pattern was established from the known heme biosynthesis pathway in *E. coli*.²² Briefly, the formation of protoheme from 5'-ALA involves seven enzymatic steps, starting with the condensation of two 5'-ALA molecules into porphobilinogen by 5'-ALA dehydratase. Interestingly, the action of uroporphyrinogen synthase circularizes the tetrapyrrole and effectively inverts the pyrrole ring corresponding to ring C in phycocyanobilin.²³ This causes the labeling of the three adjacent carbon atoms 9, 10, and 11. 5-aminolevulinic-5-¹³C acid was selected so that the C₁₉ carbon would be labeled, affecting the C₁₉=O contribution to the carbonyl region, as well as the C₁₅ methine carbon where *E,Z* isomerization is thought to take place. The complete labeling pattern includes carbon atoms C₄, C₅, C₉, C₁₀, C₁₁, C₁₅, and C₁₉ (Figure 1). Mass spectrometry showed no unlabeled material

(not shown). By inclusion of 5-amino-¹⁵N-levulinic acid in the growth medium, phytochrome with substitution of all four pyrrole nitrogen atoms with ¹⁵N isotopes was prepared. Because of the incorporation of ¹⁵N isotopes in the chromophore with the expression of Cph-N515 in the 5'-ALA auxotrophic *hemA* mutant strain in Martek 9-N media, it was not possible to prepare material labeled exclusively at the protein. The incorporation of ¹⁵N isotopes in the chromophore resulted from the presence of 5'-amino-¹⁵N-levulinic acid due to an extract from green algae that is a component of the Martek 9-N medium. To ensure uniform incorporation of ¹⁵N isotopes into both chromophore and protein, phytochrome was therefore expressed in the *hemA*+*E. coli* BL21(DE3) strain rather than in the 5'-ALA auxotrophic *hemA* mutant strain, using Martek 9-N medium in the presence of 5-amino-¹⁵N-levulinic acid. Comparison of the spectra of samples labeled exclusively with ¹⁵N in the chromophore with those from samples ¹⁵N labeled in both chromophore and protein provided a means of identification of contributions to the Pfr–Pr difference spectra of bands arising from protein.

The effects of H/D exchange, ¹³C and ¹⁵N isotope substitutions in the chromophore, and ¹⁵N isotope substitutions in the protein have allowed extension of IR assignments of the Pfr–Pr FTIR difference spectra. The major bandshifts that are discussed below are highlighted in the insets of Figures 2, 3, 4, 5, and 6. The assignments are summarized in Table 1.

Amide I and Amide II Contributions. The assignment of the large, positive feature at 1653 cm⁻¹(+) primarily to amide I and the large band at 1554 cm⁻¹(+) exclusively to amide II changes is evident from the shifts observed with H/D exchange and ¹⁵N labeling of the protein (Figures 2 and 6) cf.^{24,25} and is in agreement with a previous proposal.¹ The 1653 cm⁻¹ peak is in the region characteristic of α -helical peptide,²⁶ indicating that Pfr may be more α -helical than Pr. From integration of the

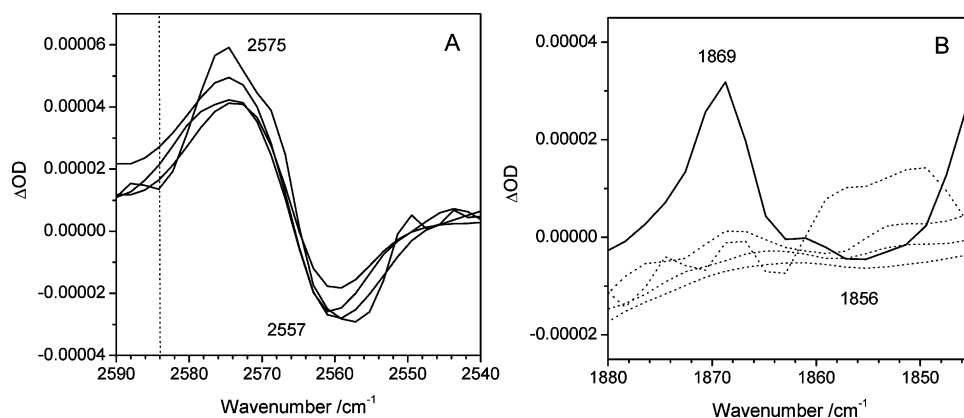


Figure 3. Cysteine perturbations: (A) high-frequency region showing S–H vibrations in H₂O, ¹³C chromophore, ¹⁵N chromophore, ¹⁵N uniform (solid traces), and D₂O (dotted trace) conditions and (B) corresponding S–D vibrations shown for D₂O (solid trace) and H₂O, ¹³C chromophore, ¹⁵N chromophore, and ¹⁵N uniform (dotted traces) conditions.

TABLE 1: Assignments of Bands of the Pfr–Pr FTIR Difference Spectra of Cph-N515 in H₂O^a

Pr(–)	Pfr(+)	assignment	references
2557	2575	Cys, ν (S–H)	
1736	1724	ν (C ₁ =O)	1,8,10,13
1734	1722	–COOH (Asp/Glu), ν (C=O)	1
1704		ν (C ₁₉ =O)	1,8,10,13
	1692	amide I (loop/turn)/propionate COOH, ν (C=O)	
1687		amide I (loop/turn)/propionate COOH, ν (C=O)	
	1683	amide I (loop/turn)/propionate COOH, ν (C=O)	
1672		amide I (loop/turn)	
	1653	amide I (α -helical)	1,8
	1653	chromophore* δ (N–H)	
	1653	chromophore* ν (C=C)	8,10
1631		amide I (β -structure)/chromophore ν (C=C)	8,12
	1614	amide I (β -structure)* /chromophore ν (C=C)	8,12
1606		amide I (β -structure)* /chromophore ν (C=C)	8,10
	1589	chromophore ν (C=C)	8,10,13
1570	1554	amide II	8,10,12,14,27,28
1537		chromophore ν (C=C) + δ (N–H)/ ν (C–N) + δ (N–H)	
1491	1512	chromophore ν (C=C) + δ (N–H)/ ν (C–N) + δ (N–H)	
1487	1502	Trp, ν (C–N) + δ (C–H) + δ (N–H)	
1246		chromophore ν (C–N)	
1244	1228	Trp*, ν (C–C) + δ (C–H)/HisH, δ (CH ₃) + ν (C–N) + δ (N–H)	
1223	1230	chromophore ν (C–N)	
	1209	chromophore ν (C–C)/amino acid	
1177	1172	chromophore ν (C–C)/amino acid	
1151	1163	chromophore ν (C–N)	
	1134	chromophore ν (C–N)	
	1119	chromophore ν (C–N)	
1109		chromophore ν (C–N)	
1107	1099	HisH, ν (C–N)	
1085	1082	chromophore ν (C–C)/amino acid	
1072		chromophore ν (C–N)	

^a When more than one contribution is proposed, they are listed as separate entries. For tentative assignments when more than one specific assignment is possible, they are listed in the same row and are separated by ‘/’. * denotes a tentative assignment. Mixing of vibrational modes is indicated with ‘+’. ν denotes stretching and δ denotes bending modes, respectively. Relevant references to specific assignments are listed in the last row.

1653 cm^{–1} difference band and the absolute amide I absorption of samples in H₂O and D₂O, the relative change of amide I absorption is estimated to be 0.25–0.5%. This relative measurement indicates that several amide bonds are affected as a result

of phototransformation of Pr to Pfr. On the basis of the D₂O and ¹³C spectra, we tentatively assign a minor part of the 1653 cm^{–1}(+) to changes of strongly hydrogen-bonded chromophore N–H bending modes and chromophore C=C modes (Table 1).

Similarly, based on the shifts observed with H/D exchange and ¹⁵N labeling of protein (Figures 2 and 6), the 1570 cm^{–1}(–)/1554 cm^{–1}(+) bands are assigned to amide II shifts. It was previously proposed that the 1567 cm^{–1}(–)/1546 cm^{–1}(+) difference band in the Pfr–Pr FTIR difference spectrum of oat phytochrome, which appears to be equivalent to the 1570 cm^{–1}(–)/1554 cm^{–1}(+) feature observed in Cph1, might correspond to the resonance Raman bands at 1568 and 1550 cm^{–1} for Pr and Pfr, respectively.^{8,10} These resonance Raman bands are known to shift down by approximately 500 cm^{–1} in D₂O and the FTIR bands in this region are also known to shift in D₂O, which has been suggested to implicate a C=NH⁺ mode including NH rocking,^{10–12,14,27,28} whereas more recent studies assigned these bands exclusively to N–H in-plane bending of rings B and C on the basis of mode calculations of the ZZZasa chromophore conformation.^{29,30} Similar bands are also observed in the resonance Raman spectra of Cph1 at 1566 and 1550 cm^{–1} for Pr and Pfr, respectively.⁶ However, the present data show unequivocally that the changes in this region of the IR spectra arise primarily from the protein amide II bandshifts rather than the chromophore bands that dominate the resonance Raman spectra in this region.

Chromophore Modes. Shifts observed with H/D exchange and ¹³C and ¹⁵N isotope substitutions in the chromophore indicate the contribution of a minimum of three components to the 1700–1750 cm^{–1} carbonyl region: the C₁=O and C₁₉=O stretch vibrations of the chromophore in addition to a protonated carboxylic acid group. Additional considerations that serve as a basis for the assignments of C=O chromophore vibrations in phytochromes are the conjugated and nonconjugated C=O vibrations, at low and high frequencies, respectively, observed in model compounds⁸ and shifts observed in the C₁=¹⁸O modified chromophore of oat phytochrome.¹³

The 1736 cm^{–1}(–)/1724 cm^{–1}(+) feature in H₂O shifts is composed of at least two components, which separate with H/D exchange and in particular with ¹⁵N labeling of the chromophore (Figures 2 and 5). These features are assigned to contributions from a protonated carboxylic acid (aspartic or glutamic acid) at 1734 cm^{–1}(–)/1722 cm^{–1}(+) and the chromophore C₁=O stretching mode at 1736 cm^{–1}(–)/1724 cm^{–1}(+). These two become better separated in the ¹⁵N chromophore labeled material, where the contribution of the newly assigned protonated carboxylic acid vibration is revealed at 1734 cm^{–1}(–)/

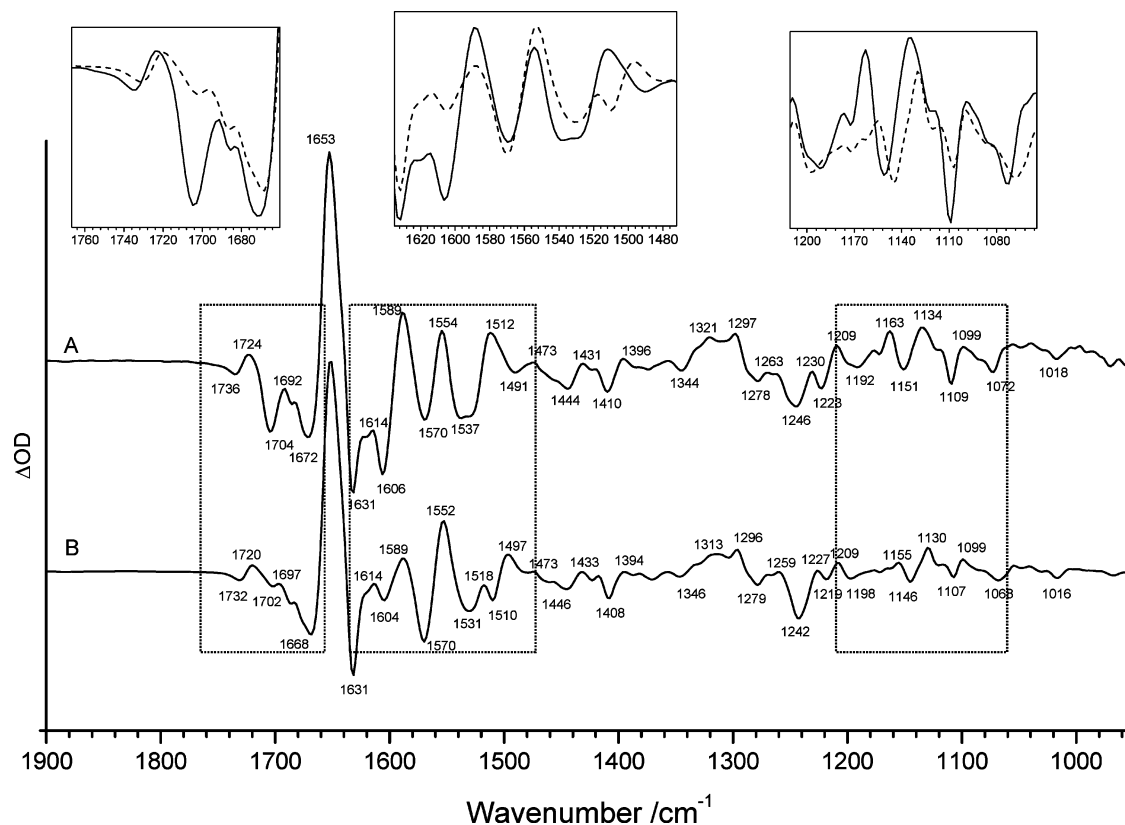


Figure 4. Shifts obtained with ^{13}C labeling of the chromophore: (A) Pfr-Pr difference spectrum of the unlabeled material in H_2O in the 950–1900 cm^{-1} region for comparison and (B) difference spectrum in H_2O of a sample containing ^{13}C isotope substitutions at the positions shown in Figure 1. Insets show overlays of the data from unlabeled material (solid line) and ^{13}C labeled material (dotted line) highlighting band position changes that are discussed.

$1722\text{ cm}^{-1}(+)$ and the $\text{C}_1=\text{O}$ stretching mode at $1714\text{ cm}^{-1}(+)$. This interpretation implies an upshift of the $\text{C}_1=\text{O}$ stretching vibration in the Pr state, corresponding to a strengthening of the $\text{C}_1=\text{O}$ bond. The $\sim 6\text{ cm}^{-1}$ downshift of this feature with H/D exchange is expected to be the result of downshifting both the $\text{C}_1=\text{O}$ stretching and the carboxylic acid bands. The downshift of the $\text{C}_1=\text{O}$ stretching mode is consistent with previous studies which showed coupling of both the $\text{C}_1=\text{O}$ and $\text{C}_{19}=\text{O}$ stretch vibrations with chromophore N-H bending modes of the oat phytochrome chromophore and linear tetrapyrrole model compounds.^{1,8,13} The $\text{C}_1=\text{O}$ mode of the phytychromobilin chromophore of oat phytochrome is found at a higher frequency, $1749\text{ cm}^{-1}(+)/1731\text{ cm}^{-1}(-)$ in H_2O , and shifts down by 5 and 9 cm^{-1} , respectively, in D_2O .¹³ The 2 cm^{-1} downshift of the $\text{C}_1=\text{O}$ mode with ^{15}N labeling of the phycocyanobilin chromophore of Cph1 (Figure 5) is also consistent with this interpretation. In the ^{13}C labeled material, the $1736\text{ cm}^{-1}(-)/1724\text{ cm}^{-1}(+)$ composite difference band shifts down by 4 cm^{-1} . Because this band is affected by ^{13}C labeling of the $\text{C}_{19}=\text{O}$, the $\text{C}_1=\text{O}$ dominated stretching mode contains some $\text{C}_{19}=\text{O}$ character. In PCB-reconstituted oat phytochrome, the $\text{C}_1=\text{O}$ stretching mode was found at a higher frequency and showed a bond strengthening in the Pfr state in contrast to Cph1.¹³ This may indicate different H-bonding properties of the PCB chromophores in the Pfr and Pr states of both phytochromes.

The 1704 cm^{-1} trough disappears with ^{13}C labeling of the chromophore, as well as with ^{15}N labeling (Figures 4 and 5) and is assigned to the $\text{C}_{19}=\text{O}$ stretching mode. It is expected that this band shifts down by approximately 40 cm^{-1} with ^{13}C labeling so it becomes masked by the large amide I band at $1653\text{ cm}^{-1}(+)$. H/D exchange causes a downshift of the $\text{C}_{19}=\text{O}$

O mode, similar to the $\text{C}_1=\text{O}$ mode (Figure 2). The assignment of 1704 cm^{-1} to $\text{C}_{19}=\text{O}$ is also in agreement with a previous proposal based on the expected frequency and intensity given its location on the D ring close to the isomerization site.¹ The band shape may be the result of a band narrowing, in which case the $\text{C}_{19}=\text{O}$ would be exposed and flexible in the Pfr state and rigid and protein bound in the Pr state.

A number of additional bands were sensitive to isotope labeling of the chromophore. Most notable with ^{13}C labeling, besides the $1736\text{ cm}^{-1}(-)/1724\text{ cm}^{-1}(+)$ and 1704 cm^{-1} band changes, were decreases in the 1589 and 1512 cm^{-1} peaks with a gain of new peaks at 1545 and 1497 cm^{-1} and band changes across the $1200\text{--}1100\text{ cm}^{-1}$ region (Figure 4). With ^{15}N labeling there were decreases of the 1589 and 1512 cm^{-1} peaks with a gain of a new peak at 1502 cm^{-1} and band changes across the $1200\text{--}1100\text{ cm}^{-1}$ region. In addition, two pronounced downshifts were found in the $1570\text{--}1475\text{ cm}^{-1}$ region (Figure 5). These data allow the identification of a range of features as the chromophore changes, including $\text{C}=\text{C}$ vibrations at $1589\text{ cm}^{-1}(+)$ and bands at $1537(-)$, $1512(+)$, $1491(-)$, $1163(+)$, $1151(-)$, $1134(+)$, $1109(-)$, and $1072(-)\text{ cm}^{-1}$ that involve chromophore C-N bonds. These chromophore bands and their tentative assignments are summarized in Table 1.

Bands at 1631 , 1614 , and 1606 cm^{-1} are mostly insensitive to ^{13}C and ^{15}N labeling of the chromophore (Figures 4 and 5) and show small downshifts with H/D exchange and ^{15}N labeling of the protein, which would be consistent with the behavior expected for amide I bands (Figures 2 and 6). In oat phytochrome, IR bands between 1610 and 1650 cm^{-1} were assigned to $\text{C}=\text{CH}-$ methine stretch vibrations, with lower frequency bands specifically assigned to ring D and the higher frequency ones to ring A,^{8,14} on the basis of the observation and assignment

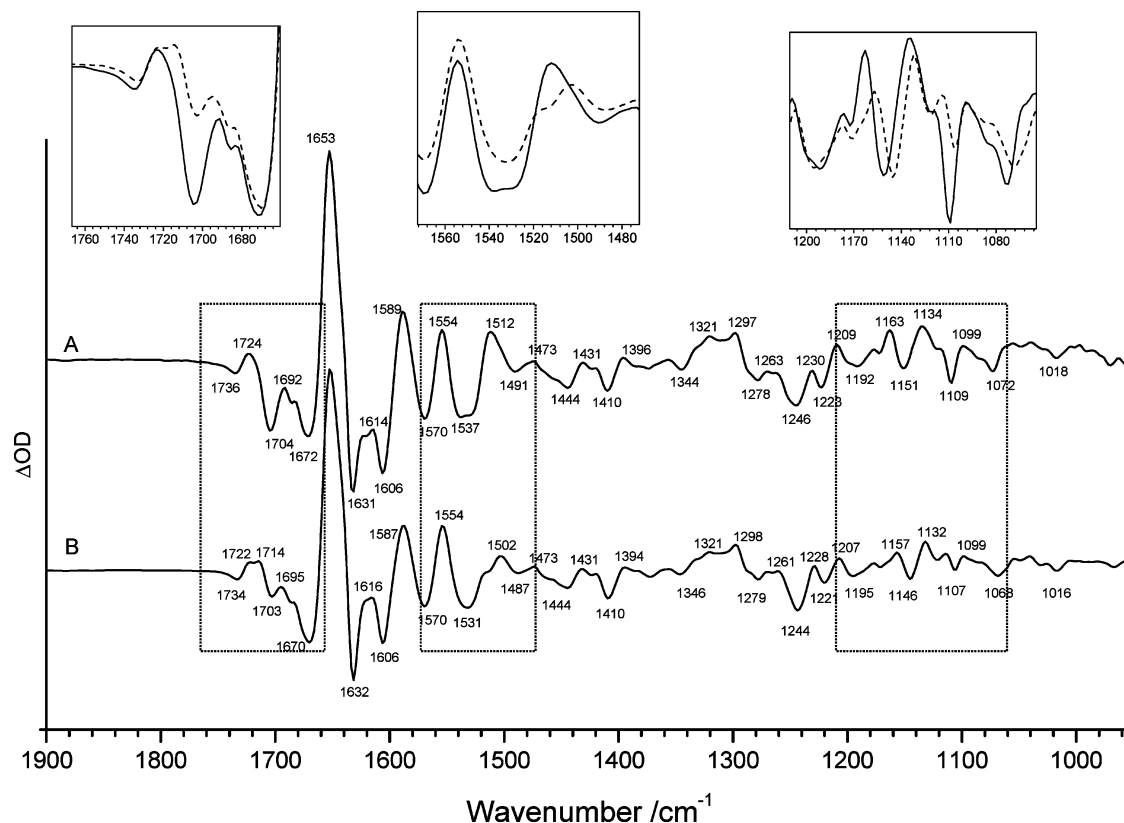


Figure 5. Shifts obtained with ^{15}N labeling of the chromophore: (A) Pfr–Pr difference spectrum of the unlabeled material in H_2O in the 950–1900 cm^{-1} region for comparison and (B) difference spectrum in H_2O of a sample containing ^{15}N isotope substitutions of the pyrrole ring nitrogen atoms of the phycocyanobilin chromophore. Insets show overlays of the data from unlabeled material (solid line) and ^{15}N chromophore labeled material (dotted line) highlighting band position changes that are discussed.

of resonance Raman bands in this region.^{12,14,31} Further, a 1614 $\text{cm}^{-1}(+)$ band in the Pfr–Pr FTIR difference spectrum of phytochromobilin-containing oat phytochrome could belong to the chromophore vinyl group.⁸ For example, the heme A vinyl group of cytochrome oxidase absorbs at 1618 cm^{-1} .³² However, in the case of Cph1, the phycocyanobilin chromophore contains an ethyl group on ring D in place of a vinyl group, excluding this assignment. Contributions in this region of the FTIR difference spectrum of Cph1 at 1631(–) and 1606(–) cm^{-1} both belong to the Pr state (Figure 2, Table 1), whereas resonance Raman bands at 1629 and 1606 cm^{-1} belong to the Pr and Pfr states, respectively.⁶ Considering this as well as the insensitivity to ^{13}C isotope labeling, bands between 1610 and 1630 cm^{-1} in the Pfr–Pr FTIR difference spectrum of Cph1 do not contain contributions from the methine bridge carbons (Figure 4) but belong to either chromophore modes that are not affected by the isotope substitution pattern (Figure 1) or possibly β -structure amide I vibrations.

Contributions of Amino Acid Residues to the Pfr–Pr Difference Spectrum. The 1734 $\text{cm}^{-1}(-)/1722 \text{ cm}^{-1}(+)$ difference band revealed with ^{15}N labeling of the chromophore is assigned to a protonated carboxylic acid residue (Figure 5). In H_2O , this is obscured by the 1736 $\text{cm}^{-1}(-)/1724 \text{ cm}^{-1}(+)$ $\text{C}_1=\text{O}$ band, though some separation is also evident in D_2O (Figure 4). The insensitivity to ^{15}N chromophore labeling in particular is consistent with a protein origin, and its frequency is characteristic for an aspartic or glutamic acid that remains in its protonated state.²⁴ This protonated carboxylic acid band may correspond to the unassigned 1739 $\text{cm}^{-1}(+)$ band which can be seen in the meta-Ra first metastable intermediate in the Pr \rightarrow Pfr pathway of Cph1.¹ The mutation of a highly conserved glutamic acid residue, E57 in Cph2, equivalent to E189 in Cph1,

abolished bilin binding,³³ and this residue could, therefore, be a candidate for the IR difference band at 1734 $\text{cm}^{-1}(-)/1722 \text{ cm}^{-1}(+)$. The pK_a of this carboxylic acid is expected to be higher than 7.8, indicating that the group is likely to be buried and does not serve as a counterion to one of the pyrrole ring B or C nitrogens, which are protonated in both Pfr and Pr states at pH 7.8.^{34,35} The downshift in Pr would indicate a decrease in H-bonding in the Pr state relative to the Pfr state.^{24,36} A recent theoretical and experimental study has provided a quantitative relationship between the frequency of the $\text{C}=\text{O}$ stretching vibrations of protonated carboxylic groups and the H-bonding strength and interactions.³⁷ This correlation predicts the H-bond energies of approximately 48 and 35 kJ/mol for the Pfr and Pr states and possibly the loss of one interaction in Pr.

When the Pfr–Pr difference spectra of the sample labeled with ^{15}N at the chromophore with that labeled in both protein and chromophore with ^{15}N isotopes are compared, several downshifts are observed outside of the amide I and amide II regions (Figure 6) and therefore must arise from amino acid changes. The 1502 $\text{cm}^{-1}(+)/1487 \text{ cm}^{-1}(-)$ difference band that is revealed in the ^{15}N chromophore labeled sample (Figure 2) is shifted down to 1497 $\text{cm}^{-1}(+)/1481 \text{ cm}^{-1}(-)$ with additional ^{15}N labeling of the protein (Figure 6). A candidate for this ^{15}N sensitive band is a vibration involving the indole C–N and N–H bonds of a tryptophan residue.^{24,36}

The bands at 1244 $\text{cm}^{-1}(-)/1228 \text{ cm}^{-1}(+)$ and 1107 $\text{cm}^{-1}(-)/1099 \text{ cm}^{-1}(+)$ are also sensitive to ^{15}N labeling of the polypeptide (Figure 6). Tryptophan is reported to have a vibration at 1245 cm^{-1} but with the main contributions from indole C–C stretch and C–H bending modes.^{24,36} A tryptophan indole vibration that contains C–N stretching is reported at 1276 cm^{-1} .^{24,36} Alternatively, these features could arise from a singly

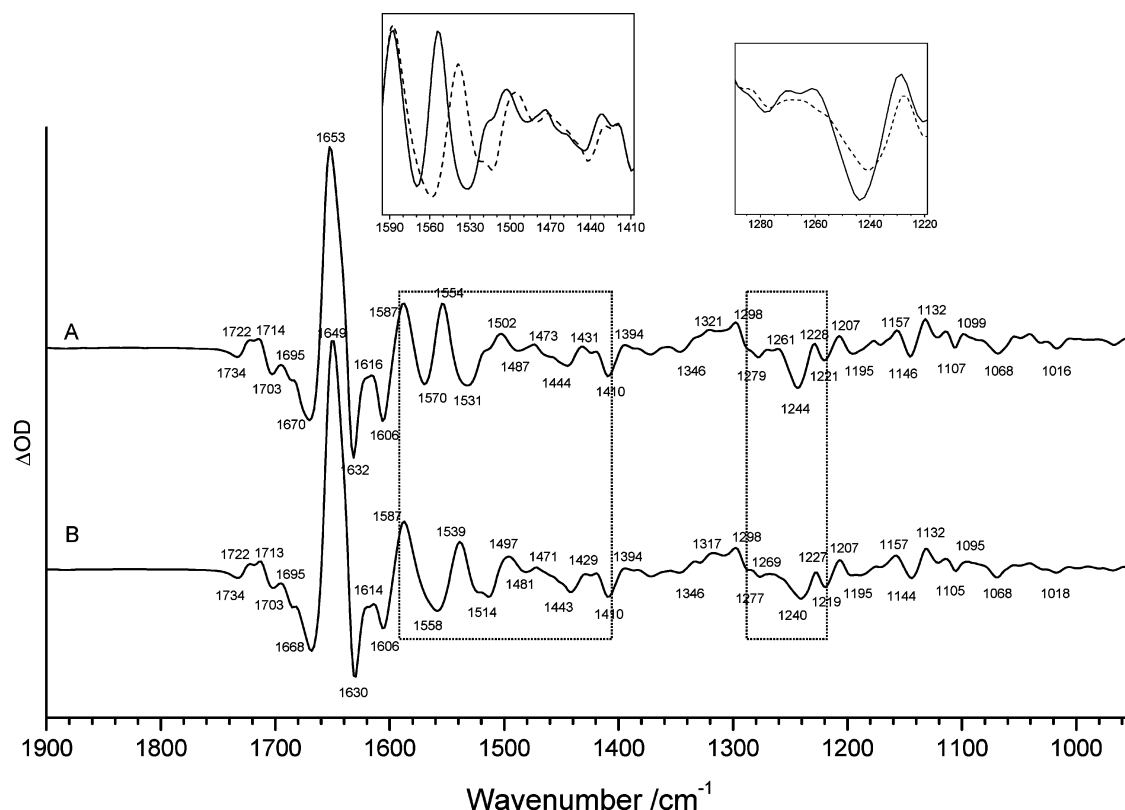


Figure 6. Shifts caused by global ^{15}N labeling of protein: (A) Pfr-Pr difference spectrum of the ^{15}N chromophore labeled sample in H_2O for comparison and (B) difference spectrum in H_2O of a sample with global ^{15}N isotope substitutions in the protein and chromophore. Insets show overlays of the data from ^{15}N chromophore labeled material (solid line) and the uniformly ^{15}N labeled material (dotted line) highlighting band position changes that are discussed.

protonated histidine undergoing an environment or protonation change.²⁴ An imidazole mode containing contributions from the $\text{N}_3\text{--C}_4$ stretch, $\text{C}_4\text{--C}_6$ stretch, and $\text{C}_5\text{--N}_1$ stretch was found at 1265 cm^{-1} in singly protonated 4-methylimidazole³⁸ and, although relatively weak, at 1262 cm^{-1} in protonated L-histidine.³⁹ Changes around 1100 cm^{-1} associated with the $\text{C}_5\text{--N}_1$ stretching mode of the imidazole ring additionally implicate histidine.³⁸

The spectral region between 1420 and 1290 cm^{-1} is mostly unaffected by the isotope substitutions at the chromophore and the protein (Figures 2, 4, 5, and 6). This suggests that other amino acid residues contribute to these signals, most probably from aliphatic residues that have weak C--H_n bands in this region. Except for one strong difference band at approximately 1410 cm^{-1} , whose origin is uncertain but could belong to a symmetric carboxylate stretching mode,²⁴ this region is also relatively featureless in the meta-Ra intermediate compared to the Pfr state,¹ which would be consistent with this interpretation.

A difference band at $2575\text{ cm}^{-1}(+)/2557\text{ cm}^{-1}(-)$ in H_2O is definitively assigned to a cysteine S--H stretching mode, showing an upshift in Pfr relative to Pr, characteristic of a decrease in H-bonding strength. The corresponding S--D stretching mode is found at $1869\text{ cm}^{-1}(+)/1856\text{ cm}^{-1}(-)$ in D_2O (Figure 3).

It was recently reported that a Y167H mutation dramatically increases the fluorescence yield of Cph1.⁴⁰ From this observation, Tyr167 was implicated directly in the phototransformation by functioning as a steric gate. Perturbation of tyrosine or tyrosinate in the $\text{Pr} \rightarrow \text{Pfr}$ transformation should result in shifts of the strong bands around 1515 or 1495 cm^{-1} , respectively.^{41,42} However, no such features are apparent. The only candidate for tyrosine in the spectra is the positive band at 1614 cm^{-1} , which shifts down to 1610 cm^{-1} in D_2O (Figure 2), which would

be consistent with shifts of the H/D sensitive band position in poly-L-tyrosine.^{41,42} However, in poly-L-tyrosine, this band is relatively weak and, combined with the lack of changes in the regions of the stronger bands in the Pfr-Pr difference spectra, the data hence provides no direct evidence that supports a role for tyrosine as a steric gate but one cannot rule out this possibility.

Structure/Function Implications. The assignments made for chromophore contributions in the Pfr-Pr difference spectra show that the chromophore structure in the holo-protein is different from model compounds, as judged from their absolute IR spectra.⁸ Bilins are known to assume helical conformations in solution⁴³ except at low pH, when all pyrrole nitrogens are protonated. The absolute absorption spectrum of purified phycocyanobilin at low pH shows little correspondence to the Pfr-Pr difference spectra. For example, phycocyanobilin shows only weak absorption at 1589 cm^{-1} (not shown) where a strong band is present in the Pfr-Pr difference spectrum (Figure 2). Upon protonation of phycocyanobilin, a strong C=C or C=N band at 1571 cm^{-1} loses most of its intensity and would be expected to shift down based on the bond order reduction. The presence of the strong C=C band at 1589 cm^{-1} in the Pfr state indicates a different structure for phytochrome-bound phycocyanobilin in the Pfr state relative to free protonated phycocyanobilin. Possibly, this mode may correspond to the ZZE-isomer-specific mode at 1602 cm^{-1} reported for protonated 2,3-dihydro-2,3,7,8,12,13,17,18-octaethyl-bilindion.⁸ The strongest indication from the assignments made to support the Z-E photoisomerization model around the $\text{C}_{15}=\text{C}_{16}$ bond is the strong band at 1704 cm^{-1} which belongs to the $\text{C}_{19}=\text{O}$ carbonyl bond. Since the $\text{C}_{19}=\text{O}$ carbonyl appears to show stronger perturbations than the $\text{C}_1=\text{O}$ bond, this may be interpreted that the D-ring is closer to the isomerization site, following previous arguments.¹ A

recent Raman and theoretical study suggests a $15Z \rightarrow E$ isomerization in the Pr \rightarrow lumi-R initial photoreaction followed by a thermal (partial) anti \rightarrow syn single bond rotation at the methine bridge between rings A and B upon formation of Pfr in plant phytochrome.¹⁴ Our extension of chromophore assignments will be helpful to interpret IR spectra in early intermediates in the photocycle from time-resolved measurements and adopt a rigorous computational approach similar to that reported for the plant phytochrome Raman work.¹⁴

The perturbation of specific amino acid side chains and the global backbone conformational changes, which are interpreted as an increased α -helical structure of Pfr relative to the Pr state, provide a picture of rearrangements of both the buried chromophore and the binding pocket of the photoreceptor protein. In particular, bands assigned to histidine (Table 1) could potentially belong to H258 and H260, which neighbor the chromophore binding C259. However, the tentative tryptophan and cysteine perturbations in the Pfr–Pr difference spectra would have to occur at more distant parts in the polypeptide. There are five candidates for the perturbed cysteine, the closest in the polypeptide chain being 30 residues C-terminal of the chromophore binding site. The assignments of features of the Pfr–Pr FTIR difference spectra to specific chromophore and protein vibrations provide a useful guide for future studies aimed at understanding structures and mechanisms of light-induced signal transduction of phytochrome photoreceptors.

Acknowledgment. This work was funded by grants from The Royal Society (University Research Fellowship to J.v.T.) and The Wellcome Trust (Grant No. 062827) to P.R.R. We acknowledge Nicolas Buisine and Ronald Chalmers for help with creating the *hemA* mutation in *E. coli* BL21(DE3).

References and Notes

- (1) Foerstendorf, H.; Lamparter, T.; Hughes, J.; Gartner, W.; Siebert, F. *Photochem. Photobiol.* **2000**, *71*, 655.
- (2) Butler, W. L.; Norris, K. H.; Siegelman, H. W.; Hendricks, S. B. *Proc. Natl. Acad. Sci. U.S.A.* **1959**, *45*, 1703.
- (3) Yeh, K. C.; Wu, S. H.; Murphy, J. T.; Lagarias, J. C. *Science* **1997**, *277*, 1505.
- (4) Franklin, K. A.; Whitelam, G. C. *J. Exp. Bot.* **2004**, *55*, 271.
- (5) Hübschmann, T.; Börner, T.; Hartmann, E.; Lamparter, T. *Eur. J. Biochem.* **2001**, *268*, 2055.
- (6) Remberg, A.; Lindner, I.; Lamparter, T.; Hughes, J.; Kneip, C.; Hildebrandt, P.; Braslavsky, S. E.; Gartner, W.; Schaffner, K. *Biochemistry* **1997**, *36*, 13389.
- (7) Rudiger, W.; Thummler, F.; Cmiel, E.; Schneider, S. *Proc. Natl. Acad. Sci. U.S.A.* **1983**, *80*, 6244.
- (8) Siebert, F.; Grimm, R.; Rudiger, W.; Schmidt, G.; Scheer, H. *Eur. J. Biochem.* **1990**, *194*, 921.
- (9) Matysik, J.; Hildebrandt, P.; Schlamann, W.; Braslavsky, S. E.; Schaffner, K. *Biochemistry* **1995**, *34*, 10497.
- (10) Foerstendorf, H.; Mummert, E.; Schafer, E.; Scheer, H.; Siebert, F. *Biochemistry* **1996**, *35*, 10793.
- (11) Andel, F., III; Lagarias, J. C.; Mathies, R. A. *Biochemistry* **1996**, *35*, 15997.
- (12) Andel, F., III; Murphy, J. T.; Haas, J. A.; McDowell, M. T.; van der Hoef, I.; Lugtenburg, J.; Lagarias, J. C.; Mathies, R. A. *Biochemistry* **2000**, *39*, 2667.
- (13) Foerstendorf, H.; Benda, C.; Gartner, W.; Storf, M.; Scheer, H.; Siebert, F. *Biochemistry* **2001**, *40*, 14952.
- (14) Mroginiski, M. A.; Murgida, D. H.; von Stetten, D.; Kneip, C.; Mark, F.; Hildebrandt, P. *J. Am. Chem. Soc.* **2004**, *126*, 16734.
- (15) Smith, K.; Matysik, J.; Hildebrandt, P.; Mark, F. *J. Phys. Chem.* **1993**, *97*, 11887.
- (16) Gambetta, G. A.; Lagarias, J. C. *Proc. Natl. Acad. Sci. U.S.A.* **2001**, *98*, 10566.
- (17) Munson, M.; Predki, P. F.; Regan, L. *Gene* **1994**, *144*, 59.
- (18) Nakayashiki, T.; Nishimura, K.; Tanaka, R.; Inokuchi, H. *Mol. Gen. Genet.* **1995**, *249*, 139.
- (19) Kolter, R.; Inuzuka, M.; Helinski, D. R. *Cell* **1978**, *15*, 1199.
- (20) Glasoe, P. K.; Long, F. A. *J. Phys. Chem.* **1960**, *64*, 188–190.
- (21) Rath, P.; DeGrip, W. J.; Rothschild, K. J. *Biophys. J.* **1998**, *74*, 192.
- (22) Panek, H.; O'Brian, M. R. *Microbiology* **2002**, *148*, 2273.
- (23) Battersby, A. R. *Experientia* **1978**, *34*, 1.
- (24) Barth, A.; Zscherp, C. *Q. Rev. Biophys.* **2002**, *35*, 369.
- (25) Susi, H. In *Structure and stability of biological macromolecules*; Timasheff, S. N., Stevens, L., Eds.; Dekker: New York, 1969; pp 575–663.
- (26) Luis, J. R.; Muga, A. A.; Castresana, J.; Goñi, F. M. *Prog. Biophys. Mol. Biol.* **1993**, *59*, 23.
- (27) Fodor, S. P.; Lagarias, J. C.; Mathies, R. A. *Photochem. Photobiol.* **1988**, *48*, 129.
- (28) Fodor, S. P.; Lagarias, J. C.; Mathies, R. A. *Biochemistry* **1990**, *29*, 11141.
- (29) Kneip, C.; Hildebrandt, P.; Nemeth, K.; Mark, F.; Schaffner, K. *Chem. Phys. Lett.* **1999**, *311*, 479.
- (30) Kneip, C.; Hildebrandt, P.; Schlamann, W.; Braslavsky, S. E.; Mark, F.; Schaffner, K. *Biochemistry* **1999**, *38*, 15185.
- (31) Margulies, L.; Toporowicz, M. *J. Am. Chem. Soc.* **1984**, *106*, 7331.
- (32) Berthomieu, C.; Boussac, A.; Mantele, W.; Breton, J.; Navedryk, E. *Biochemistry* **1992**, *31*, 11460.
- (33) Wu, S. H.; Lagarias, J. C. *Biochemistry* **2000**, *39*, 13487.
- (34) van Thor, J. J.; Borucki, B.; Crielgaard, W.; Otto, H.; Lamparter, T.; Hughes, J.; Hellingwerf, K. J.; Heyn, M. P. *Biochemistry* **2001**, *40*, 11460.
- (35) Strauss, H. M.; Hughes, J.; Schmieder, P. *Biochemistry* **2005**, *44*, 8244.
- (36) Barth, A. *Prog. Biophys. Mol. Biol.* **2000**, *74*, 141.
- (37) Nie, B.; Stutzman, J.; Xie, A. *Biophys. J.* **2005**, *88*, 2833.
- (38) Hasegawa, K.; Ono, T.; Noguchi, T. *J. Phys. Chem. B* **2000**, *104*, 4253.
- (39) Iwaki, M.; Yakovlev, G.; Hirst, J.; Osyczka, A.; Dutton, P. L.; Marshall, D.; Rich, P. R. *Biochemistry* **2005**, *44*, 4230.
- (40) Fischer, A. J.; Lagarias, J. C. *Proc. Natl. Acad. Sci. U.S.A.* **2004**, *101*, 17334.
- (41) Rothschild, K. J.; Roepe, P.; Ahl, P. L.; Earnest, T. N.; Bogomolni, R. A.; Das Gupta, S. K.; Mulliken, C. M.; Herzfeld, J. *Proc. Natl. Acad. Sci. U.S.A.* **1986**, *83*, 347.
- (42) Rich, P. R.; Iwaki, M. In *Biophysical and Structural Aspects of Bioenergetics*; Wikstrom, M., Ed.; Royal Society of Chemistry: Cambridge, U.K., 2005; Chapter 13, pp 314–333.
- (43) Krois, D. *Monatsh. Chem.* **1991**, *122*, 495.